

Full nonuniversality of the symmetric 16-vertex model on the square lattice

Eva Pospíšilová, Roman Krčmár, Andrej Gendiar, and Ladislav Šamaj

Institute of Physics, Slovak Academy of Sciences, Dúbravská cesta 9, 84511 Bratislava, Slovakia

(Dated: March 2, 2022)

We consider the symmetric two-state 16-vertex model on the square lattice whose vertex weights are invariant under any permutation of adjacent edge states. The vertex-weight parameters are restricted to a critical manifold which is self-dual under the gauge transformation. The critical properties of the model are studied numerically by using the Corner Transfer Matrix Renormalization Group method. The accuracy of the method is tested on two exactly solvable cases: the Ising model and a specific version of the Baxter 8-vertex model in a zero field. The numerical results imply parameter-dependent critical exponents which clearly violate weak universality hypothesis.

I. INTRODUCTION

According to the universality hypothesis [1], critical exponents of a statistical system at the second-order phase transition do not depend on details of the corresponding Hamiltonian. Equivalently, critical exponents depend only on system's space dimensionality and symmetry of microscopic degrees of freedom (say spins). The first violation of the universality hypothesis was observed in the Baxter's exact solution of the 8-vertex model on the square lattice in a zero electric field [2–4] whose critical exponents are functions of the model parameters. Suzuki [5] argued that the violation of universality in the 8-vertex model is due to the identification of the deviation from the critical point with the temperature difference $|T_c - T|$. Instead, if taking the inverse correlation length $|T_c - T|^\nu$ (the critical exponent ν is assumed to be the same for both limits $T \rightarrow T_c^-$ and $T \rightarrow T_c^+$) as the natural measure of the distance from the critical point, the renormalized exponents $\beta/\nu, \gamma/\nu, \delta = 1 + \frac{\gamma}{\beta}$, etc. become universal, i.e. independent of model's parameters. This phenomenon is known as weak universality. Weak universality was observed in many two-dimensional (2D) systems, including the Ashkin-Teller model [6–8], absorbing phase transitions [9], the spin-1 Blume-Capel model [10], frustrated spin models [11, 12], percolation models [13], etc. There are few exceptions from models with continuously varying critical exponents which violate weak universality, such as micellar solutions [14], Ising spin glasses [15], itinerant composite magnetic materials [16, 17], etc.

The partition function of the “electric” 8-vertex model on the square lattice can be mapped onto the partition function of a “magnetic” Ising model on the dual (also square) lattice with nearest-neighbor two-spin and plaquette four-spin interactions [18, 19]. Baxter's solution of the zero-field 8-vertex model [2, 3] implies in fact all magnetic critical exponents obeying weak universality, but only one electric critical exponent (namely β_e which describes the temperature singularity of the spontaneous polarization). Recently two of us [20] argued that the critical exponents related to the divergence of the correlation length must coincide in both magnetic and electric formats: $\nu_e = \nu$.

Having at one's disposal two critical exponents, all other electric exponents have been derived by using scaling relations. The obtained analytic formulas for the electric critical exponents are in perfect agreement with numerical results obtained by the Corner Transfer Matrix Renormalization Group method. It turns out that the model's variation of the electric critical exponents violates weak universality. Thus although the partition functions of the electric and magnetic model's versions are equivalent, their critical properties are fundamentally different: while the magnetic critical exponents obey weak universality, the electric ones do not and therefore they are fully nonuniversal.

The partition function of a vertex model is invariant under gauge transformation of vertex weights [21, 22] which is a generalization of the weak-graph expansion [23] and the duality transformation. If a point in the parameter space of vertex weights is mappable onto itself by a nontrivial gauge transformation, it belongs to the self-dual manifold where critical points of second-order phase transitions lie.

The model under consideration in this paper is the symmetric two-state 16-vertex models on the square lattice whose vertex weights are isotropic, i.e. invariant under any permutation of adjacent edge states. This model was introduced in Ref. [24] in connection with the $O(2)$ gauge transformation which preserves the permutation symmetry of vertex weights and its self-dual manifolds can be found relatively simply. In a certain subspace of vertex weights, the model can be mapped onto Ising spins in a field [25, 26]. The critical properties of the model were studied numerically by combining a series expansion on the lattice and the Coherent Anomaly method [27] in Ref. [28]. In spite of modest computer facilities and lack of efficient numerical methods at that time (almost 30 years ago), the numerical results indicate the full nonuniversality of the model. For a recent survey of the general 16-vertex model with an enlargement of known mappings, see Ref. [29].

The aim of this work is to revisit the study of the electric critical properties of the symmetric of the 16-vertex model on the square lattice by using the Corner Transfer Matrix Renormalization Group (CTMRG) method [30–34]. The method is based on the renormalization of the density matrix [35–37] and the

technique of corner transfer matrices [3]. It has been applied to many 2D lattice models and provides very accurate results for critical points and exponents. The present work confirms with a high reliability that the symmetric 16-vertex on the square lattice is nonuniversal and violates the weak universality hypothesis.

The paper is organized as follows. The definition and basic facts about the model, including the gauge transformation of vertex weights, are given in Sec. II. Two exactly solvable cases are discussed: the Ising model and a specific version of the Baxter eight-vertex model in zero field. The CTMRG method is reviewed briefly in Sec. III. Numerical results for the critical temperatures and exponents are presented in IV. Sec. V brings a short recapitulation and concluding remarks.

II. MODEL AND ITS EXACTLY SOLVABLE CASES

A. Basic facts about the model

The general two-state vertex model on the square lattice of N ($N \rightarrow \infty$) sites is defined as follows. Each lattice edge can be in one of two states. These states will be denoted either by \pm signs or by “dipole” arrows: the right/up oriented arrow corresponds to the (+) state, while the left/down arrow to the (−) state. With each vertex we associate the set of 2^4 possible Boltzmann weights $w(s_1, s_2, s_3, s_4) = \exp[-\varepsilon(s_1, s_2, s_3, s_4)/T]$. In units of $k_B = 1$, both energy $\varepsilon(s_1, s_2, s_3, s_4)$ and temperature T are taken as dimensionless. For the symmetric version of the model, the vertex weights are invariant with respect to any permutation of state variables (s_1, s_2, s_3, s_4) . Let us denote by $w_i = \exp(-\varepsilon_i/T)$ ($i = 0, 1, \dots, 4$) the vertex weight with i incident edges in the (−) state and the remaining $4 - i$ incident edges in the (+) state. Thus from among 16 possible configurations of vertex states there is 1 corresponding to each of the vertex weights w_0 and w_4 , 4 corresponding to each of w_1 and w_3 and 6 corresponding to w_2 , see Fig. 1.

Thermal equilibrium of the system is determined by the (dimensionless) free energy per site

$$-\frac{f(\{w\})}{T} = \lim_{N \rightarrow \infty} \frac{1}{N} \ln Z(\{w\}), \quad (1)$$

where

$$Z(\{w\}) = \sum_{\{s\}} \prod_{\text{vertex}} (\text{weights}), \quad (2)$$

is the partition function with the summation going over all possible edge configurations and the product being over all vertex weights in the lattice. The mean concentration c_i of the vertices with weight w_i is given

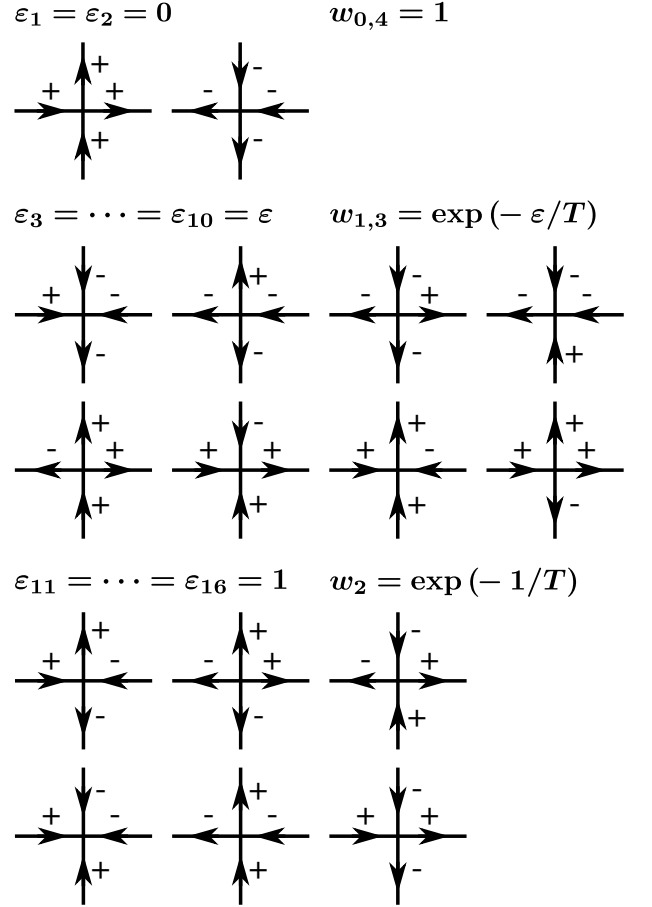


FIG. 1. Vertex weights of the symmetric 16-vertex model on the square lattice, invariant with respect to the flip of all adjacent edge states $+ \leftrightarrow -$.

by

$$c_i = -w_i \frac{\partial}{\partial w_i} \frac{f(\{w\})}{T} \quad (i = 0, \dots, 4). \quad (3)$$

The mean concentrations are constrained by the obvious normalization condition $\sum_{i=0}^4 c_i = 1$. The mean-value of the edge-state variable

$$P = \frac{1}{4} \sum_{i=0}^4 (4 - 2i) c_i \quad (4)$$

defines the polarization. When one applies an isotropic electric field E (with the same strength along either of the two axis), each arrow dipole $s = \pm 1$ gets the energy $-Es$. Since every dipole belongs to just two vertices, the vertex weights are modified to

$$w_i(E) = w_i \exp[E(2 - i)/T]. \quad (5)$$

One can trivially extend the definitions of the vertex concentrations (3) and the polarization (4) to $E \neq 0$,

with the corresponding notations $c_i(E)$ and $P(E)$. Then the polarization susceptibility reads as

$$\chi = \lim_{E \rightarrow 0} \frac{\partial P(E)}{\partial E} = \frac{1}{2} \sum_{i,j=0}^4 (2-i)(2-j) \chi_{ij}, \quad (6)$$

where

$$\chi_{ij} = -\frac{\partial}{\partial \epsilon_j} c_i(E=0) \quad (7)$$

form the tensor of generalized susceptibilities.

The partition function of the general two-state vertex model is invariant under the $O(2)$ gauge transformation of vertex weights [21, 22]. For the square lattice with the coordination number 4, the gauge transformation reads as

$$\begin{aligned} \tilde{w}(s_1, s_2, s_3, s_4) = & \sum_{s'_1, s'_2, s'_3, s'_4} V_{s_1 s'_1}(y) V_{s_2 s'_2}(y) V_{s_3 s'_3}(y) \\ & \times V_{s_4 s'_4}(y) w(s'_1, s'_2, s'_3, s'_4). \end{aligned} \quad (8)$$

Here, $V_{ss'}(y)$ are the elements of the matrix

$$\mathbf{V}(y) = \frac{1}{\sqrt{1+y^2}} \begin{pmatrix} 1 & y \\ y & -1 \end{pmatrix} \quad (9)$$

with rows (columns) indexed from up to down (left to right) as $+, -$ and a free (real) gauge parameter y . For the symmetric version of the vertex model, the gauge transformation keeps the permutation symmetry of vertex weights [24], namely

$$\tilde{w}_i = \sum_{j=0}^4 W_{ij}(y) w_j \quad (i = 0, 1, \dots, 4), \quad (10)$$

$$W_{ij}(y) = \frac{1}{(1+y^2)^2} \sum_{k=0}^{\min(i,j)} \binom{i}{k} \binom{4-i}{j-k} (-1)^k y^{i+j-2k}. \quad (11)$$

Points in the vertex-weight parameter space which can be mapped onto itself by gauge transformation with a nontrivial (point-dependent) value of $y \neq 0$, form the so-called self-dual manifold. The self-dual manifold for the symmetric 16-vertex model is given by [24]

$$\begin{aligned} w_0^2 w_3 - w_1 w_4^2 - 3w_2(w_0 - w_4)(w_1 + w_3) \\ + (w_1 - w_3)[w_0 w_4 + 2(w_1 + w_3)^2] = 0. \end{aligned} \quad (12)$$

Its importance consists in the fact that critical points of second-order phase transitions are confined to this subspace of vertex weights.

In this work, we restrict ourselves to the symmetric 16-vertex model whose vertex weights are invariant with respect to the flip of all adjacent edge states $(+) \leftrightarrow (-)$. The vertex weights are parametrized as follows

$$w_0 = w_4 = 1, \quad w_1 = w_3 = e^{-\epsilon/T}, \quad w_2 = e^{-1/T}, \quad (13)$$

see also Fig. 1, where the real parameter $\epsilon \geq 0$. It can be checked that this choice of vertex weights automatically satisfy the self-dual condition (12). Thus for a fixed value of the energy ϵ there should exist a critical temperature T_c at which a second-order phase transition takes place. In the disordered phase at $T > T_c$, the state-flip symmetry ensures that the equality of concentrations $c_i = c_{4-i}$, so that the mean polarization (4) vanishes. In the ordered phase at $T < T_c$, the state-flip symmetry breaking causes that $c_i \neq c_{4-i}$ and the spontaneous polarization P becomes nonzero. Close to T_c , it is the non-analytic function of $T_c - T$:

$$P \propto (T_c - T)^{\beta_e}, \quad T \rightarrow T_c^- \quad (14)$$

with β_e (the subscript e means “electric”) being the critical exponent. Applying to the vertex system a small isotropic external electric field E just at the critical temperature, the polarization behaves as

$$P(E) \propto E^{1/\delta_e}, \quad T = T_c, \quad (15)$$

where δ_e is another critical exponent. Close to the critical point, the polarization susceptibility (6) exhibits the singularity of type

$$\chi \propto \frac{1}{|T_c - T|^{\gamma_e}}, \quad (16)$$

where the critical exponent γ_e is assumed to be the same for both limits $T \rightarrow T_c^-$ and $T \rightarrow T_c^+$. The pair arrow-arrow correlation function exhibits the large-distance behavior

$$G_e(r) \propto \frac{1}{r^{\eta_e}} \exp(-r/\xi), \quad r \rightarrow \infty. \quad (17)$$

Close to the critical point, the correlation length ξ behaves as

$$\xi \propto \frac{1}{|T_c - T|^{\nu_e}}. \quad (18)$$

The divergence of ξ at $T = T_c$ reflects the fact that the short-range (exponential) decay out of the critical point changes to the long-range (inverse power-law) one at $T = T_c$ characterized by the critical exponent η_e .

Having at one's disposal two critical exponents β_e and δ_e , the remaining ones (considered in this work) can be calculated by using scaling relations [3]:

$$\begin{aligned} \gamma_e &= \beta_e (\delta_e - 1), \\ \nu_e &= \frac{1}{2} \beta_e (\delta_e + 1), \\ \eta_e &= \frac{4}{\delta_e + 1}. \end{aligned} \quad (19)$$

B. Ising point

The symmetric 16-vertex model can be mapped onto an Ising model on the square lattice if the vertex weights are constrained by [25, 26]

$$w_0 w_2 w_4 - w_0 w_3^2 - w_1^2 w_4 + 2w_1 w_2 w_3 - w_2^3 = 0. \quad (20)$$

For the state-flip symmetry of vertex weights (13), this equation takes the form

$$1 + e^{1/T} = 2e^{2(1-\varepsilon)/T}. \quad (21)$$

As concerns the parameters of the Ising model for the state-flip symmetry, the external magnetic field acting on spins $H = 0$ and the (dimensionless) coupling J between nearest-neighbor spins is given by

$$J = \frac{1}{2} \ln \left(\frac{w_1}{w_2} \right) = \frac{1 - \varepsilon}{2T}. \quad (22)$$

The known critical value of the Ising coupling reads [3]

$$J_c = \frac{1}{2} \ln (1 + \sqrt{2}). \quad (23)$$

Consequently, Eqs. (21) and (22) imply the following critical parameters of the symmetric 16-vertex model:

$$\varepsilon^{(1)} = 1 - \frac{\ln(1 + \sqrt{2})}{\ln(5 + 4\sqrt{2})} = 0.627516\dots, \quad (24)$$

$$T_c^{(1)} = \frac{1}{\ln(5 + 4\sqrt{2})} = 0.422618\dots \quad (25)$$

In contrast to standard mappings of models on dual lattices, the mapping between the symmetric 16-vertex and Ising models is made on the *same* square lattice [25, 26]. The relation between the polarization of the symmetric 16-vertex model and the magnetization of the equivalent Ising system can be derived by using the technique presented in Ref. [38]. This relation is linear and therefore the critical exponents of the symmetric 16-vertex model coincide with the Ising ones. The Ising critical exponents are summarized in Table I.

exponent	β_e	δ_e	γ_e	ν_e	η_e
$\varepsilon^{(1)} \approx 0.6275$	1/8	15	7/4	1	1/4
$\varepsilon \rightarrow \infty$	1/8	11	5/4	3/4	1/3

TABLE I. List of electric critical exponents for the symmetric 16-vertex model at the exactly solvable Ising and the Baxter 8-vertex points.

C. 8-vertex point

When $\varepsilon \rightarrow \infty$, the vertex configurations w_1 and w_3 in Fig. 1 with odd numbers of (+), or equivalently (−), edge states vanish. The consequent Baxter's 8-vertex model has vertex-weight parameters $a = w_0 = w_4 = 1$ and $b = c = d = w_2 = \exp(-1/T)$ [3]. The vertex system exhibits the ferroelectric-A phase for $a > b + c + d$. The second-order transition between the ferroelectric-A and disordered phases takes place at

$$a_c = b_c + c_c + d_c, \quad T_c = \frac{1}{\ln 3} = 0.910239\dots \quad (26)$$

Introducing the auxiliary parameter

$$\mu = 2 \arctan \left(\sqrt{\frac{a_c b_c}{c_c d_c}} \right) = \frac{2\pi}{3}, \quad (27)$$

according to Ref. [20] the electric critical exponents are given by

$$\begin{aligned} \beta_e &= \frac{\pi - \mu}{4\mu} = \frac{1}{8}, \\ \delta_e &= \frac{3\pi + \mu}{\pi - \mu} = 11, \\ \gamma_e &= \frac{\pi + \mu}{2\mu} = \frac{5}{4}, \\ \nu_e &= \frac{\pi}{2\mu} = \frac{3}{4}, \\ \eta_e &= 1 - \frac{\mu}{\pi} = \frac{1}{3}. \end{aligned} \quad (28)$$

These critical exponents are summarized in Table I.

III. NUMERICAL METHOD

The CTMRG method [30–32] is based on Baxter's technique of corner transfer matrices [3]. Each quadrant of the square lattice with size $L \times L$ is represented by the corner transfer matrix C . The reduced density matrix is defined by $\rho = \text{Tr}' C^4$ (where the partial trace Tr' is taken), so that the partition function $Z = \text{Tr} \rho$, see Fig. 2. The number of degrees of freedom grows exponentially with L and the density matrix is used in the process of their reduction. Namely, degrees of freedom are iteratively projected to the space generated by the eigenvectors of the reduced density matrix ρ with the largest eigenvalues. The projector on this reduced space of dimension m will be denoted by O ; the larger truncation parameter m is taken, the better precision of the results is attained. In each iteration the linear system size is expanded from $2L$ to $2L + 2$ via the inclusion of the Boltzmann weight W of the basic vertex (see Fig. 1). The expansion process transforms the corner transfer matrix C to C' and the half-row transfer matrix H to H' in the way represented schematically in Fig. 2. The

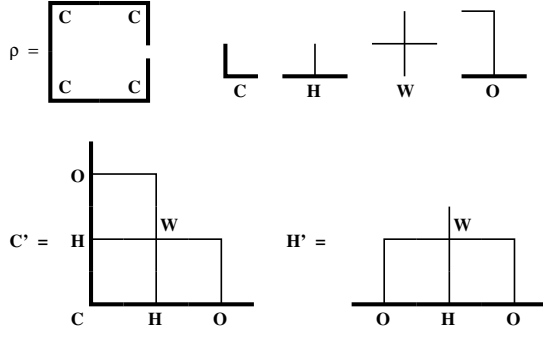


FIG. 2. The CTMRG renormalization process. The density matrix ρ is composed of four transfer matrices C . The expansion process of the corner transfer matrix $C \rightarrow C' = O^\dagger H W C H O$ and the half-row transfer matrix $H \rightarrow H' = O^\dagger H W O$ from the previous iteration RG Step, see the text.

thick lines (lines) represent renormalized multi-arrow (arrow) variables obtained after the renormalization which consists in the summation and O -projection of multi-arrow (arrow) thick lines (lines) from the previous iteration. The fixed boundary conditions are used, with each arrow at the boundary line set to the value $s = -1$. This choice ensures a quicker convergence of the method in the ordered phase towards the thermodynamic limit.

IV. NUMERICAL RESULTS

According to Eq. (14), the critical temperature T_c is the lowest temperature at which $P = 0$ or, equivalently, the highest temperature at which $P \neq 0$. Based on comparison with the known values of the Ising (25) and Baxter's (26) critical temperatures, the error in estimation of $T_c(\varepsilon)$ is of order 10^{-4} for all values of ε . The error is even smaller (of order 10^{-5}) when fitting data for the spontaneous polarization close to the critical point according to (14). Numerical results for the ε -dependence of the critical temperature are shown in Fig. 3. We see that $T_c(\varepsilon)$ is only weakly affected by dimension of the truncated space $m = 100$ and $m = 200$.

The inset of Fig. 3 documents the log-log plot of the small- ε behavior of $T_c(\varepsilon)$. The power-law least-square fitting at low $\varepsilon < 10^{-8}$ yields

$$T_c(\varepsilon) = -6.6 \times 10^{-18} + 0.954(5)\varepsilon^{0.9998(3)}, \quad (29)$$

where the absolute term is on the accuracy border of the computer. We conclude that in the limit of small ε the critical temperature converges to zero linearly. On the other hand, as ε increases the critical temperature saturates quickly to the value 0.91024 which is close to the asymptotic $\varepsilon \rightarrow \infty$ analytic result (26) of the 8-vertex model.

The critical exponent β_e should interpolate between the same values $1/8$ at small and large ε . It is calculated again by fitting polarization data according to formula

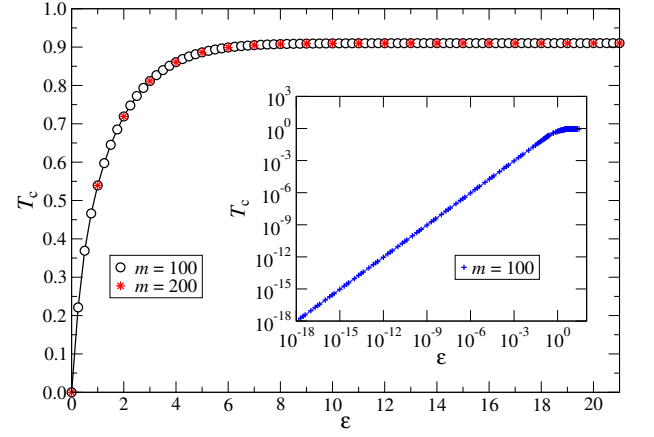


FIG. 3. The ε -dependence of the critical temperature T_c of the symmetric 16-vertex model, for dimension of the truncated space $m = 100$ (open circles) and $m = 200$ (open circles with stars). The inset shows a linear dependence of $T_c(\varepsilon)$ for small values of ε .

(14). With T_c fixed in the previous calculation, we have selected a series of temperatures below threshold value $T_c - 0.0002$ with a temperature step ΔT at which the polarization is evaluated. For each value of ε , we have generated 6 polarization values with $\Delta T = 10^{-4}$ and 30 polarization values with $\Delta T = 10^{-5}$, taking dimension of the truncated space $m = 100$ and $m = 200$. The corresponding ε -dependences of the critical exponent β_e within the range of $\varepsilon \in [0, 25]$, are pictured in Fig. 4. We see that the too small value of the temperature step $\Delta T = 10^{-5}$ and $m = 100$ (triangles) leads in the region of large values of ε incorrectly to $\beta_e > 1/8$. Increasing method's accuracy to $m = 200$ (diamonds), data converge to the correct value $\beta_e = 1/8$ at large ε . On the other hand, for a larger temperature step $\Delta T = 10^{-4}$, both $m = 100$ (circles) and $m = 200$ (squares) data are consistent with $\beta_e = 1/8$ at large ε . We conjecture that the optimal parameters are $\Delta T = 10^{-4}$ and $m = 200$; other plots are presented in Fig. 4 only to judge the accuracy of relevant square data. In the short interval of $\varepsilon \lesssim 2$ containing the Ising point $\varepsilon = 0.627516\dots$, the exponent is roughly constant $\beta_e = 1/8$. In the interval $2 \lesssim \varepsilon \lesssim 14$, β_e varies non-monotonously as function of ε . For $\varepsilon \gtrsim 14$, the exponent β_e is again roughly constant and acquires its Baxter's $\varepsilon \rightarrow \infty$ value $\beta_e = 1/8$ as it should be.

The critical exponent δ_e is expected to interpolate between the values 15 at small ε and 11 at large ε . It is calculated by fitting polarization data at the critical temperature T_c according to the relation (15) which can be rewritten as

$$\delta_e = \left(\frac{\partial \ln P}{\partial \ln E} \right)^{-1}. \quad (30)$$

This formula has to be considered for a very small value

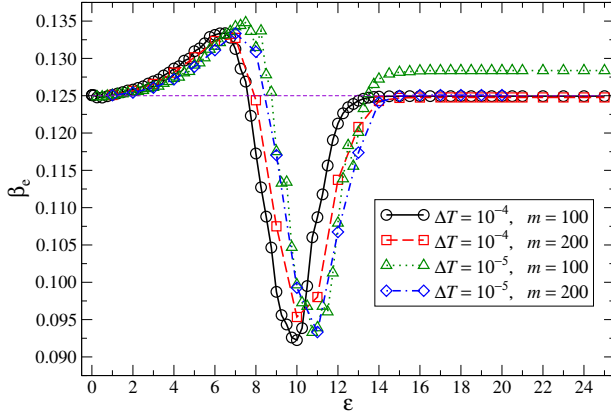


FIG. 4. The ε -dependence of the critical exponent β_e for the symmetric 16-vertex model with the temperature steps $\Delta T = 10^{-4}$ and 10^{-5} and dimensions of the truncated space $m = 100$ and $m = 200$.

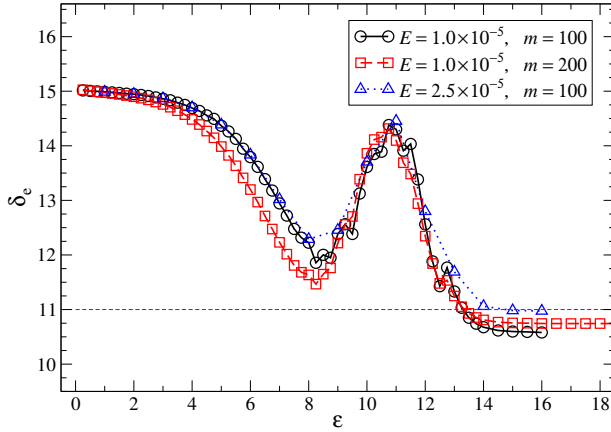


FIG. 5. The ε -dependence of the critical exponent δ_e for the symmetric 16-vertex model. Data are generated for the electric field $E = 10^{-5}$ at approximation orders $m = 100$ (circles) and $m = 200$ (squares), and the optimal $E = 2.5 \times 10^{-5}$ at $m = 100$ (triangles).

of field E , but not too small to avoid numerical errors due to the critical state of the vertex system. The obtained data for $E = 10^{-5}$ and 2.5×10^{-5} are presented in Fig. 5, within the range of $\varepsilon \in [0, 18]$. Data for $E = 10^{-5}$, evaluated at approximation orders $m = 100$ (circles) and $m = 200$ (squares), converge well below the anticipated value 11. On the other hand, numerical data for the optimal field $E = 2.5 \times 10^{-5}$ evaluated at approximation order $m = 100$ (triangles) are lying close to the previous data for $E = 10^{-5}$ with $m = 200$ and for large values of $\varepsilon \gtrsim 14$ tend correctly to the value 11.

The critical exponent γ_e is expected to interpolate between $7/4$ at small ε and $5/4$ at large values of ε . This exponent is calculated by fitting the susceptibility data according to the formula (16). Fitting is performed in the region $T > T_c$ with the susceptibility functional values

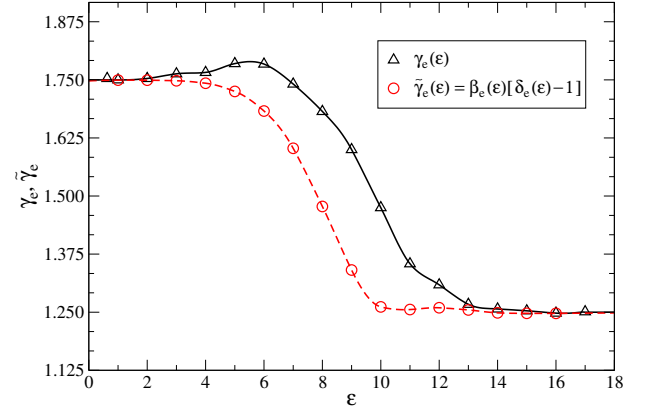


FIG. 6. The ε -dependence of the critical exponent γ_e for the symmetric 16-vertex model. Data are generated from fitting of the formula (16), in the region $T > T_c$ and the susceptibility values $\chi \in [10000, 50000]$ calculated with dimension of the truncated space $m = 100$ (triangles). The exponent $\tilde{\gamma}_e$, calculated by inserting the previous data for β_e and δ_e into the first of scaling relations (19), is represented by circles.

from the interval $\chi \in [10000, 50000]$. Within the range of $\varepsilon \in [0, 18]$, the obtained $m = 100$ data are represented by triangles in Fig. 6. Data tend for small and large values of ε correctly to $7/4$ and $5/4$, respectively. Because fits of the singular formula (16) are accompanied by relatively large errors, we have calculated alternatively $\tilde{\gamma}_e$ by inserting the previous data for β_e and δ_e into the first of scaling relations (19). Hereinafter, we adopt convention that an exponent deduced by using scaling relations will be denoted by a tilde on its top. Numerical data for $\tilde{\gamma}_e$ are represented in Fig. 6 by circles. Note that the plot exhibits a monotonous decay.

The critical exponents $\tilde{\nu}_e$ and $\tilde{\eta}_e$, calculated by inserting the previous data for β_e and δ_e into the second and third of scaling relations (19), respectively, are represented as functions of ε in Fig. 7 by triangles and circles, respectively. Both plots exhibit non-monotonous behavior. The exponent $\tilde{\nu}_e$ interpolates correctly between 1 at small ε and $3/4$ at large ε and $\tilde{\eta}_e$ interpolates correctly between $1/4$ at small ε and $1/3$ at large ε .

As seen in Figs. 4-7, the critical exponents of the symmetric 16-vertex model on the square lattice depend on model's parameter ε . To judge the validity of the hypothesis of weak universality, note that the critical points and exponents of the exactly solvable Ising $\varepsilon^{(1)} \approx 0.6275$ and Baxter's $\varepsilon \rightarrow \infty$ cases lie on the same continuous curve. It is therefore sufficient to test the renormalized exponents β_e/ν_e , γ_e/ν_e and the exponent δ_e , which are independent of model's parameters if weak universality works, at the two exactly solvable points. In

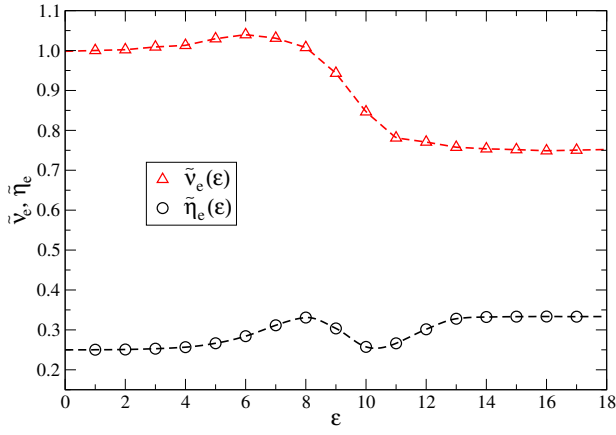


FIG. 7. The critical exponents $\tilde{\nu}_e$ (triangles) and $\tilde{\eta}_e$ (circles), calculated by inserting the previous data for β_e and δ_e into the second and third of scaling relations (19), respectively, as functions of $\varepsilon \in [0, 18]$.

particular, from Table I we have

$$\frac{\beta_e}{\nu_e} = \begin{cases} \frac{1}{8} & \varepsilon^{(1)} \approx 0.6275, \\ \frac{1}{6} & \varepsilon \rightarrow \infty, \end{cases} \quad (31)$$

$$\frac{\gamma_e}{\nu_e} = \begin{cases} \frac{7}{4} & \varepsilon^{(1)} \approx 0.6275, \\ \frac{5}{3} & \varepsilon \rightarrow \infty, \end{cases} \quad (32)$$

$$\delta_e = \begin{cases} 15 & \varepsilon^{(1)} \approx 0.6275, \\ 11 & \varepsilon \rightarrow \infty. \end{cases} \quad (33)$$

We conclude that weak universality hypothesis is violated in the present model, i.e. the symmetric 16-vertex model on the square lattice is fully nonuniversal.

V. CONCLUSION

The system under consideration in this paper was the symmetric two-state 16-vertex model on the square lattice. Its vertex weights, which are invariant under any permutation of adjacent edge states, are considered to be symmetric with respect to the flip of all adjacent edge states $(+) \leftrightarrow (-)$ (see Fig. 1) as well. Such vertex weights automatically lie on the self-dual manifold of the gauge transformation (12), carrying critical points. The parametrization of vertex weights (13) contains two positive parameters, the temperature T and the energy ε . Two exactly solvable cases, namely the Ising model and the specific version of Baxter's 8-vertex model correspond to $\varepsilon^{(1)} \approx 0.6275$ and $\varepsilon \rightarrow \infty$, respectively. To study critical properties of the model, we have applied the very accurate CTMRG method. The dependence of the critical temperature T_c on ε is pictured in Fig. 3. The fit of the plot in the region of small ε (see the inset) indicates the linear dependence with T_c going to 0 as $\varepsilon \rightarrow 0$. The plot of the critical exponent β_e versus ε , calculated with optimal parameters of the temperature step $\Delta T = 10^{-4}$ and dimension of the reduced space $m = 200$, is represented by square data in Fig. 4. The critical exponent $\delta_e(\varepsilon)$ is calculated with optimal parameters of the electric field $E = 2.5 \times 10^{-5}$ and $m = 100$, see triangle data in Fig. 5. The plots of the exponent γ_e versus ε are evaluated “from first principles” (triangles) and by using the first of scaling relations (19) (circles) in Fig. 6. The dependence of the critical exponents ν_e and η_e on ε , evaluated by using the second and third of scaling relations (19), are presented in Fig. 7. All critical exponents interpolate correctly between their known values at the two solvable cases $\varepsilon^{(1)} \approx 0.6275$ and $\varepsilon \rightarrow \infty$. The variation of the critical exponents with model's parameter ε is such that weak universality hypothesis is violated.

ACKNOWLEDGMENTS

The support received from the project EXSES APVV-16-0186 and VEGA Grants Nos. 2/0003/18 and 2/0123/19 is acknowledged.

-
- [1] R. B. Griffiths, Phys. Rev. Lett. **24**, 1479 (1970).
 - [2] R. J. Baxter, Phys. Rev. Lett. **26**, 832 (1971).
 - [3] R. J. Baxter, *Exactly Solved Models in Statistical Mechanics*, (Academic Press, London, 1982).
 - [4] L. Šamaj and Z. Bajnok, *Introduction to the Statistical Physics of Integrable Many-body Systems* (Cambridge University Press, Cambridge, 2013).
 - [5] M. Suzuki, Prog. Theor. Phys. **51**, 1992 (1974).
 - [6] J. Ashkin and E. Teller, Phys. Rev. **64**, 178 (1943).
 - [7] L. P. Kadanoff, Phys. Rev. Lett. **39**, 903 (1977).
 - [8] A. B. Zisook, J. Phys. A: Math. Gen. **13**, 2451 (1980).
 - [9] J. D. Noh and H. Park, Phys. Rev. E **69**, 016122 (2004).
 - [10] A. Malakis, A. N. Berker, I. A. Hadjiagapiou, and N. G. Fytas, Phys. Rev. E **79**, 011125 (2009).
 - [11] S. L. A. de Queiroz, Phys. Rev. E **84**, 031132 (2011).
 - [12] S. Jin, A. Sen, and A. W. Sandvik, Phys. Rev. Lett. **108**, 045702 (2012).
 - [13] R. F. S. Andrade and H. J. Herrmann, Phys. Rev. E **88**, 042122 (2013).
 - [14] M. Corti, V. Degiorgio, and M. Zulauf, Phys. Rev. Lett. **48**, 1617 (1982).

- [15] L. Bernardi and I. A. Campbell, Phys. Rev. B **52**, 12501 (1995).
- [16] D. Fuchs et al. Phys. Rev. B **89**, 174405 (2014).
- [17] N. Khan, P. Sarkar, A. Midya, P. Mandal, and P. K. Mohanty, Sci. Rep. **7**, 45004 (2017).
- [18] F. Y. Wu, Phys. Rev. B **4**, 2312 (1971).
- [19] L. P. Kadanoff and F. J. Wegner, Phys. Rev. B **4**, 3989 (1971).
- [20] R. Krčmár and L. Šamaj, Phys. Rev. E **97**, 012108 (2018).
- [21] F. J. Wegner, Physica **68**, 570 (1973).
- [22] A. Gaaff and J. Hijmans, Physica A **80**, 149 (1975).
- [23] J. F. Nagle, J. Math. Phys. **9**, 1007 (1968).
- [24] X. N. Wu and F. Y. Wu, J. Phys. A: Math. Gen. **22**, L55 (1989).
- [25] L. Šamaj and M. Kolesík, Mod. Phys. Lett. B **5**, 1075 (1991).
- [26] L. Šamaj and M. Kolesík, Physica A **182**, 455 (1992).
- [27] M. Suzuki, J. Phys. Soc. Jpn. **55**, 4205 (1986).
- [28] M. Kolesík and L. Šamaj, J. Stat. Phys. **72**, 1203 (1993).
- [29] M. Assis, J. Phys. A: Math. Theor. **50**, 395001 (2017).
- [30] T. Nishino and K. Okunishi, J. Phys. Soc. Jpn. **65**, 891 (1996).
- [31] T. Nishino and K. Okunishi, J. Phys. Soc. Jpn. **66**, 3040 (1997).
- [32] K. Ueda, R. Otani, Y. Nishio, A. Gendiar, and T. Nishino, J. Phys. Soc. Jpn. **74**, 1871 (2005).
- [33] R. Krčmár and L. Šamaj, Europhys. Lett. **115**, 56001 (2016).
- [34] J. Genzor, T. Nishino, and A. Gendiar, Acta Phys. Slov. **67**, 85 (2017).
- [35] S. R. White, Phys. Rev. Lett. **69**, 2863 (1992).
- [36] S. R. White, Phys. Rev. B **48**, 10345 (1993).
- [37] U. Schollwöck, Rev. Mod. Phys. **77**, 259 (2005).
- [38] M. Kolesík and L. Šamaj, Physica A **179**, 145 (1991).